Mon. Not. R. Astron. Soc. **000**, 000–000 (0000) Printed 29 January 2013 (MN LATEX style file v2.2)

A coherent acceleration search of the Parkes multi-beam pulsar survey - techniques and the discovery and timing of 16 pulsars

R. P. Eatough[1,2⋆], M. Kramer[1,2], A. G. Lyne[2] and M. J. Keith[3]
[1] *Max-Planck-Institut für Radioastronomie, Auf dem Hügel 69, 53121, Bonn, Germany.*
[2] *Jodrell Bank Centre for Astrophysics, Alan Turing Building, University of Manchester, Manchester, M13 9PL, United Kingdom.*
[3] *Australia Telescope National Facility, CSIRO Astronomy & Space Science, PO Box 76, Epping, NSW 1710, Australia.*

1 May 2008

ABSTRACT
A fully coherent acceleration search algorithm has been applied to the Parkes multi-beam pulsar survey of the Galactic plane to search for previously undiscovered relativistic binary pulsars. The search has resulted in the discovery of 16 pulsars including a binary millisecond pulsar and an intermittent pulsar. Despite a number of promising candidates there have been no new discoveries of relativistic binary pulsars. Here we detail the acceleration search performed in our analysis and present coherent timing solutions for each of pulsars discovered. In light of the lack of discoveries of relativistic binary pulsars, we also discuss the technique of acceleration searching and its effectiveness in finding these systems.

Key words: methods: data analysis - pulsars: general - stars: neutron

1 INTRODUCTION

Radio pulsars in compact, highly-relativistic binary systems, such as double neutron star systems (DNS) and pulsar white dwarf systems (NS-WD), provide the most precise tests of Einstein's theory of General Relativity (GR) and alternative theories of gravity in the strong-field regime (e.g. Taylor & Weisberg 1989, Kramer et al. 2006, Breton et al. 2008, Freire et al. 2012). Future more stringent tests of gravity could be performed with more compact and/or higher-mass systems such as pulsar-black hole binary systems (NS-BH) (Kramer et al. 2004), or even pulsars orbiting closely around the super massive black hole at the centre of the Galaxy, Sgr A⋆ (Pfahl et al. 2005, Liu et al. 2012). The increased orbital velocities and deeper gravitational potentials present in such systems would result in larger post-Keplerian (PK) orbital effects, which are measurable through pulsar timing (Damour & Esposito-Farèse 1998, Wex & Kopeikin 1999).

Searches for these highly-prized systems are notoriously difficult. After correction for the frequency dependent dispersion in the arrival time of pulses, caused by the unknown free electron content along the line-of-sight ('dedispersion'), standard pulsar searches look for significant features in the fluctuation spectrum of the dedispersed time series (see, for example, Lorimer & Kramer 2005, for a detailed description of pulsar search methods). In relativistic binary systems, Doppler smearing of the pulse frequency, caused by rapid orbital motion during the survey observation, renders standard Fourier-based pulsar search algorithms ineffective (see, e.g. Johnston & Kulkarni 1991). The binary search algorithms that compensate for these effects are computationally expensive in blind pulsar searches. Hence, the analysis of large-scale pulsar surveys, like the Parkes multi-beam pulsar survey (PMPS), have not yet been performed with optimum binary searches (Faulkner et al. 2004). In this work we have attempted to further combat binary selection effects in the Parkes multi-beam pulsar survey by re-processing the entire survey with an efficient 'coherent acceleration search'.

The outline of the rest of this paper is as follows: In Section 2, we give a summary of the PMPS and describe previous binary searches of the survey data. Section 3 is a description of the binary search algorithm employed in this search. In Section 4, details of the re-processing data pipeline are given. Section 5 presents timing solutions of all 16 pulsars and further details on any of the notable discoveries. Section 6 provides a discussion of possible reasons for the lack of discoveries of any new relativistic binaries in addition to further tests of the acceleration algorithm presented here. Section 7 is a summary and a discussion of future work on searches for relativistic binary pulsars.

⋆ E-mail: reatough@mpifr-bonn.mpg.de

2 THE PARKES MULTI-BEAM PULSAR SURVEY

The PMPS is the most successful pulsar survey ever completed, having discovered 770 pulsars up to the start of this work (Manchester et al. 2001, Morris et al. 2002, Kramer et al. 2003, Hobbs et al. 2004, Faulkner et al. 2004, Lorimer et al. 2006, Keith et al. 2009) and over 30 pulsars discovered by their single pulses (McLaughlin et al. 2006, Keane et al. 2010, Keane et al. 2011). The survey was carried out between 1997 and 2003 using a 13-beam receiver with a bandwidth of 288 MHz centred on 1374 MHz and deployed on the 64-m Parkes radio telescope in Australia. It covers a strip along the Galactic plane from $l = 260^\circ$ to $l = 50^\circ$ and $|b| < 5^\circ$ with time series of 35 minutes digitally sampled every 250 μs. Full details of the survey can be found in Manchester et al. (2001).

2.1 Previous binary searches

Despite the early successes of the PMPS the number of compact binary pulsars (orbital period, $P_\mathrm{b} < 1$ day) and millisecond pulsars (spin period, $P < 30$ ms) discovered was low; one and three respectively (Table 3.2, Faulkner 2004). The long integration time of 35 minutes gave the PMPS unprecedented sensitivity to long-period pulsars, although, in searches for relativistic binary pulsars, where the spin frequency can change over the duration of the observation, sensitivity was lost in standard Fourier periodicity searches due to smearing of the spectral features of the pulsar.

After an improvement in computational resources at the Jodrell Bank Observatory, in the form of the COBRA 182-node Beowulf cluster, a full re-processing of the PMPS was performed using two search algorithms designed to address the previously-described binary selection effects (Faulkner 2004, Faulkner et al. 2004). The algorithms used in this analysis were the 'stack-slide search' (see, for example, Wood et al. 1991) and the 'phase modulation search' (Ransom et al. 2003). In the stack-slide search technique each dedispersed time series is split into a number of contiguous segments (16 in the case of the PMPS re-processing), which are Fourier transformed separately. The resulting fluctuation spectra are then summed together with different linear offsets to correct for linear drift in pulse frequency caused by any constant line-of-sight acceleration. So called 'acceleration searches' have been shown to be valid for observations where the integration time, T_obs, is $\lesssim P_\mathrm{b}/10$ (Ransom et al. 2003). For the PMPS this corresponded to binary systems with $P_\mathrm{b} \gtrsim 6$ hr.

The phase modulation search works by detecting "periodic sidebands" in the fluctuation spectrum; the common marker of a pulsar in a binary system (Ransom et al. 2003). Pulsars in binary systems where at least 1.5 orbits are completed during the observation time can be detected with this technique. For the PMPS this corresponded to systems with $P_\mathrm{b} \lesssim 0.4$ hr.

The Faulkner et al. (2004) reprocessing found 11 binary pulsars including the double neutron star system, PSR J1756−2251, that would not have been discovered without the stack-slide search (Faulkner et al. 2005). Of the other 10 binary systems, three were detected with higher significance because of the stack-slide search (on average by a factor of ~ 1.9: Table 7.2, Faulkner 2004). Results from the phase modulation search have never been fully inspected due to difficulties in reconstructing the predicted orbit of pulsar candidates (Faulkner, private communication).

Although the stack-slide search method improved sensitivity to pulsars in some fast binary systems, sensitivity was lost due to the incoherent summation of spectra. By splitting the time series into a number of segments, each of which is Fourier transformed and then summed, the phase coherence of any real signal is not preserved throughout the entire length of the observation. In the presence of Gaussian noise, and assuming stacks of equal length, the signal-to-noise ratio (S/N) of a real signal increases $\propto \sqrt[4]{n}$ where n is the number of spectra stacked (Brady & Creighton 2000). As already noted, the stack-slide and phase modulation searches left a gap in sensitivity for pulsars in binary systems with P_b between ~ 0.4 and ~ 6 hr. For systems that lie in this region of parameter space, sensitivity might also have been lost because of observed changes in acceleration ('jerk') that the linear offsets applied in the stack-slide search cannot compensate for. Both the orbital-period sensitivity gap and the reduction in sensitivity due to the incoherent nature of the stack search might have been critical in the detection of a relativistic binary pulsar that was near the detection threshold of the survey. In this work we describe further efforts to tackle binary selection effects in the PMPS.

3 A COHERENT ACCELERATION SEARCH ALGORITHM, PMACCN

It is possible to perform acceleration searches in the time domain that are fully coherent and without the loss of sensitivity encountered in stacking algorithms. One such technique is 'time domain resampling'; a method that enabled the discovery of nine binary millisecond pulsars in observations of 47 Tucanae at 20-cm (Camilo et al. 2000). Following the description in Section 2 of Camilo et al. (2000), the time series is transformed into a frame which is inertial with respect to the pulsar by application of the Doppler formula to relate a time interval in the pulsar frame τ to the time interval in the observed frame t,

$$\tau(t) = \tau_0 \left(1 + v(t)/c\right), \tag{1}$$

where $v(t)$ is the changing line-of-sight velocity of the pulsar, c is the speed of light, and the constant τ_0 is chosen such that τ is equivalent to the sampling interval, τ_samp at the midpoint of the observation. New samples are computed from a linear interpolation over the original time series (Middleditch & Kristian 1984). Following resampling, the time series can be searched with standard Fourier techniques, as if the pulsar were isolated (see for example Lorimer & Kramer 2005). To fully remove the effects of orbital motion, the exact form of $v(t)$ must be known, although in a blind search, where the orbital elements are a priori unknown, this would require a search over five Keplerian parameters; a task that would require significant computational resources (see for example, Dhurandhar & Vecchio 2001, and discussion in Appendix A). To reduce the amount of computation required, the assumption of a constant line-of-sight acceleration, a, can once again be applied, so that $v(t) = at$. Now, searches in just

one parameter, constant line-of-sight acceleration, a, can be made, but in a fully coherent manner.

A step size between each acceleration trial, δa was determined by fixing the amount of signal advance or retardation with respect to either end of the integration[1] to a value that was deemed acceptable. This value, which we shall now term 'pulse broadening', $\tau_{\rm accn}$, was chosen to be four times the sampling interval, $\tau_{\rm samp}$, i.e. if the pulsar signal fell between two acceleration trials this would be the maximum value of pulse broadening at the end points of the data. Because of the quadratic nature of the pulse broadening with time, due to a constant acceleration, a (see for example Equation 4 in Johnston & Kulkarni 1991),

$$\tau_{\rm accn}(t) = at^2/2c, \tag{2}$$

at least 50 per cent of pulses in the integration would be smeared in time by less than one time sample. Setting the pulse broadening time, given by Equation 2, equal to $8\,\tau_{\rm samp}$ allows a maximum of $4\,\tau_{\rm samp}$ pulse smearing for signals that lie exactly in-between acceleration trials. Remembering that resampling is performed with respect to the midpoint of the data, $t = T_{\rm obs}/2$, giving the acceleration step size, δa:

$$\delta a = 64c\tau_{\rm samp}/T_{\rm obs}^2. \tag{3}$$

Our choice of acceleration step size is illustrated in Figure 1. Here we plot the pulse phase as a function of time for an idealized top hat pulse that has a width equal to a single sample, and that is accelerated to a value that is directly in between acceleration trials. The pulse phase broadening at the end points of the integration is therefore $4\,\tau_{\rm samp}$; the maximum value it can take. For a broadening of $4\,\tau_{\rm samp}$ at the end points it can be seen that 50 per cent of the pulses are smeared in phase by less than $\tau_{\rm samp}$. Although the total broadening time is less than $\tau_{\rm samp}$ for half of the observation, the majority of power in a sample will be smeared into the next sample when, for example, $\tau_{\rm accn} > 0.5\,\tau_{\rm samp}$, which occurs after $T_{\rm obs}/\sqrt{32}$ using this step size.

The acceleration step size given in Equation 3 scales linearly with the sampling interval and with inverse square of the integration time. Longer integrations and smaller sample intervals therefore require finer acceleration steps. Both of these parameters could be tuned within the limits of the PMPS data to find an optimum acceleration step size which covered new regions of parameter space without excessive levels of computation. The final processing parameters of our search algorithm, termed PMACCN, are given in Table 1. Data processing benchmarks and algorithm performance tests described in Eatough (2009)[2] favoured a search based on two independent half segments of the original 35 minute integration, and a sampling interval increased by a factor of four from the original 250 μs to 1 ms. Using this choice of processing parameters a wide range of accelerations ($\pm 500\,{\rm m\,s^{-2}}$) could be searched in a manageable time on the computational hardware available (see Section 4). The acceleration range chosen is nearly twice the maximum acceleration present in the most relativistic binary pulsar known: the Double Pulsar system ($\sim 260\,{\rm m\,s^{-2}}$: Burgay et al. 2003,

[1] The effect of the constant, τ_0 in Equation 1 is such that resampling is performed with respect to the midpoint of the observation.
[2] www.jb.man.ac.uk/∼reatough/reatough_thesis.pdf

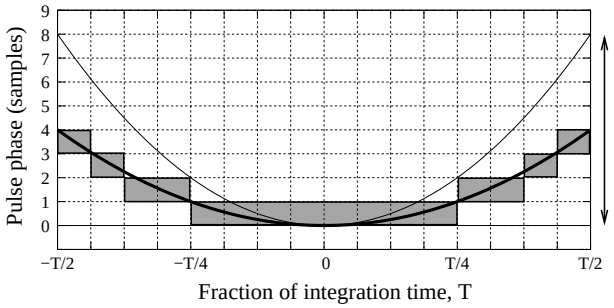

Figure 1. Time versus pulse phase for an idealized top hat pulse with a width equal to the sampling interval (dark grey blocks) and a true acceleration, indicated by the thick black line, that lies directly in between acceleration trials given by Equation 3 (thin black lines). Arbitrary time intervals are marked by the vertical dotted lines. The size of the acceleration step is indicated by the vertical arrow on the right. For signals that have a true acceleration that lies in between acceleration trials, at least 50 per cent of the pulses are smeared by less than $\tau_{\rm samp}$.

Table 1. PMACCN processing parameters. The step size in dispersion measure (DM) was determined following standard procedures outlined in Lorimer & Kramer (2005). The range in DM searched was defined by the expected values in the Galactic plane given by the Cordes & Lazio (2002) free electron density model of the Galaxy. Each data segment corresponds to one independent half of the original 35 minute integration.

Parameter	Value
Integration time	2×1050 s
Sample interval	1 ms
Number of samples per data segment	2^{20}
Size of the data segments	49 MB
Acceleration search range	± 500 m s^{-2}
Number of acceleration trials	59
DM search range	0−1656 cm^{-3}pc
Number of DM trials	152
Processing time (per data segment)	$\sim$ 2.25 hr
Total number of data segments	2×34710

Kramer et al. 2006) and is a value that might be expected in compact NS-BH systems (see Section 6). Analyzing independent halves also provided better sensitivity to more compact binary systems ($P_{\rm b} \gtrsim 3$ hr) that would have been missed by acceleration searches of the full length observation, because of the effects of jerk (e.g. $P_{\rm b} \gtrsim 6$ hr in Faulkner et al. 2004). The sampling interval of 1 ms was not optimal for millisecond pulsars, however it is expected that in most NS-BH systems the pulsar will be the second-born object and will not have undergone recycling (Sipior et al. 2004).

Understanding the response of the data processing system to incorrect acceleration trials is important for validating both genuinely accelerated and even solitary pulsar candidates. The full effects of a constant line-of-sight acceleration on the integrated pulse S/N can be examined if we consider a simple Gaussian pulse convolved with the pulse broadening function given by Equation 2. In Figure 2, the bottom panel shows the signal advance or retard due to a number of constant accelerations within the 1050 s of the PMACCN search algorithm. The thin black lines represent

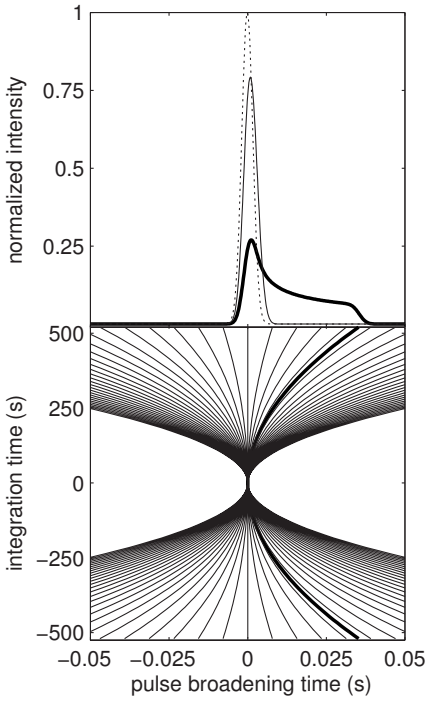

Figure 2. The bottom panel shows the signal advance or retard due to a number of constant accelerations. The thin black lines represent accelerations for which the data can be corrected using the resampling method. The step size between acceleration trials is that given by Equation 3, for a sample interval of 1 ms and an integration time of 1050 s, as in the PMACCN search algorithm. In this case the simulated pulsar signal has an acceleration of 78.3 m s^{-2} and falls in the middle of two acceleration trials (thick black line). The upper panel shows the effect of the pulse broadening on a simulated Gaussian pulse for a pulsar with a spin period of 50 ms and a pulse width of 10 per cent. The dotted line shows the original pulse profile, with no broadening; the thick black line shows the profile broadening caused by the acceleration and the thin black line shows the "acceleration-corrected" profile for acceleration trials closest to the true acceleration.

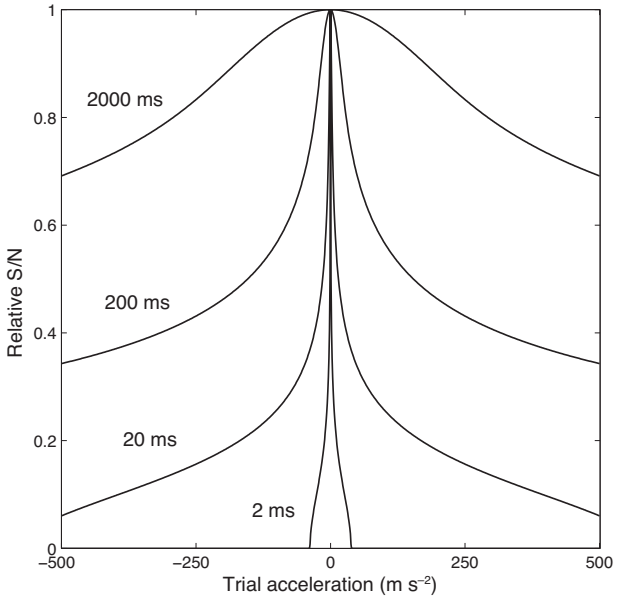

Figure 3. Relative pulse S/N variation with incorrect acceleration trial for a range of pulsar periods. In all cases the pulse duty cycle is five per cent, and the signal has a true acceleration of 0 m s^{-2}.

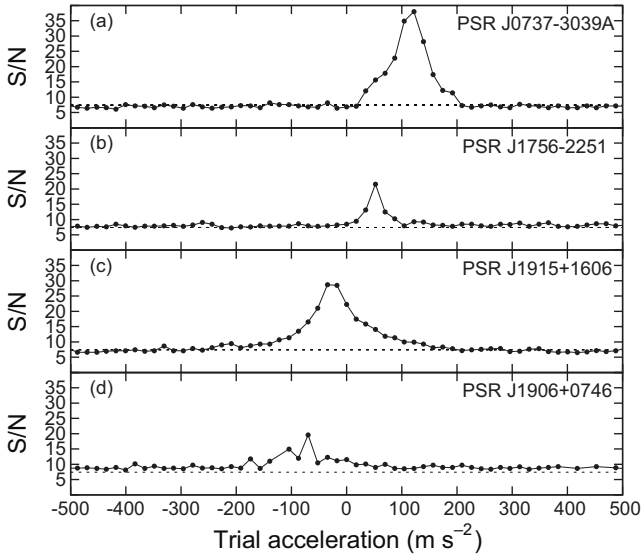

Figure 4. Spectral S/N as a function of trial acceleration for four known relativistic binary pulsars using the PMACCN search algorithm. The horizontal dotted lines (at S/N = 7.4) show the minimum value of S/N considered not to be from the effects of statistical noise, based on the false-alarm probability (e.g. Lorimer & Kramer 2005).

accelerations that can be compensated for using acceleration steps based on Equation 3. Here we plot the "worst case" scenario where a true signal from a pulsar, accelerated to 78.3 m s^{-2}, shown by the thick black line, lies exactly in the middle of two acceleration trials. If resampling is performed with respect to the midpoint of the data then the maximum pulse broadening is 4 ms. In the top panel we plot the effects of the pulse broadening on a simulated Gaussian pulse from a pulsar with a spin period of 50 ms and a pulse width of 10 per cent. The dotted line shows the original pulse profile with no acceleration effects. The thick black line shows the full effects of the pulse broadening caused by acceleration and the thin black line shows the 'acceleration-corrected' profile. The reduction in pulse amplitude, caused by broadening, depends on the intrinsic width of the pulse i.e. assuming an constant duty cycle, shorter period pulsars will experience increased broadening compared to longer period pulsars. In Figure 3 we show how the pulse S/N (related to the effective width and period of the pulse, see e.g. Lorimer & Kramer (2005) page 129) changes with incorrect acceleration trial for a number of pulse periods, ranging from two milliseconds to two seconds. In these examples the pulse duty cycle is fixed at five per cent and the actual acceleration of the signal is 0 m s^{-2}. Shorter period pulsars are smeared by incorrect acceleration trials more quickly than their longer period counterparts. As well as showing the importance of correcting for pulse broadening caused by constant accelerations, the curves displayed in Figure 3 provide a useful diagnostic for genuinely accelerated pulsar signals.

3.1 Algorithm tests

The PMACCN acceleration search algorithm has been tested on observations of a number of known relativistic binary pulsars, and using data from simulations of compact DNS and NS-BH systems (Eatough 2009). Post facto tests of the algorithm, described in Section 6.3, have also been performed. The results from tests on real observations of relativistic binary pulsars are presented in Figure 4. Each panel shows the spectral S/N, from the fluctuation spectrum, as a function of trial acceleration for 1050 s integrations with the PMPS observing system. PSR A in the Double Pulsar system is shown in panel (a) and is found at an acceleration of 122 m s^{-2}. Panel (b) shows PSR J1756−2251, detected at an acceleration of 52 m s^{-2}. In panel (c) the binary pulsar, B1913+16 is found with an acceleration of −26 m s^{-2}. Finally panel (d) shows the binary pulsar J1906+0746 detected at −70 m s^{-2}. Standard non-accelerated pulsar searches would give spectral S/Ns roughly equal to the value in the 0 m s^{-2} acceleration trial. In these tests the PMACCN acceleration search increases the spectral S/Ns by a factor of between at least two and five compared to a standard non-accelerated pulsar search. However, this improvement is dependent upon the orbital phase at which the pulsar was observed and is discussed in more detail in Section 6.

4 THE PROCESSING

It was estimated that processing the PMPS using the acceleration algorithm described in Section 3 would require an order of magnitude more computational operations than the Faulkner et al. (2004) processing used. An opportunity arose to use the computing facilities of The University of Manchester, High Energy Physics (HEP) group. Their TIER2 computing facility[3] consists of 900 dual-core nodes that form part of a network of high-performance computers for the analysis of particle physics data from the Large Hadron Collider, known as GridPP[4]. GridPP was built by a collaboration of 19 UK universities, the Rutherford Appleton Laboratory and Conseil Européen pour la Recherche Nucléaire (CERN). The UK's GridPP is connected to a much wider global collaboration of computing centres called the Worldwide LHC Computing Grid[5] and in total provides the equivalent computing power of approximately 200,000 CPUs. One of the primary aims of computational grids, such as GridPP, is to exploit and share the computational power available from disparate sets of computers or computer clusters that are connected by the Internet. Such 'grid' based distributed computing lends itself well to the highly-parallel nature of processing the data from pulsar surveys.

4.1 Data processing overview

Data processing was divided into two main stages. Firstly 'local' processing, where the PMPS pointings were separated into 13 individual beams and each integration divided into two halves on the Jodrell Bank Centre for Astrophysics (JBCA) DCORE computer cluster. This was followed by 'external' beam processing, where each half integration was acceleration-searched on the TIER2 facility. The flow of data and processing steps from acquisition at the telescope up to the inspection of pulsar candidates generated from the search is depicted in Figure 5.

In summary, the PMPS data were stored in pointings of 13 independent beams on a RAID system at the JBCA. Each data file consists of 2^{23} single-bit samples for each of the 96 3-MHz-wide frequency channels. The raw data were first separated into 13 individual beams using a dedicated FORTRAN program, SC_TD. Each beam was then converted into multi-channel SIGPROC format, for use with the SIGPROC pulsar processing suite[6], and split into two 1050 s segments. Each of the half-length integrations was stored on the JBCA RAID system, ready for processing on the TIER2 facility. These initial processing tasks were performed on the DCORE computer cluster, to avoid excessive levels of data transfer to the TIER2 facility.

The submission of processing jobs to the TIER2 facility was controlled by the 'user interface' to GridPP: a linux desktop machine located at the JBCA. Processing jobs were submitted to the TIER2 'gatekeepers'; machines that maintained a batch queue of jobs. Once a processing job started on a TIER2 worker node, a request was sent to a JAVA control program, running at the JBCA, that kept a queue of un-processed data files. When a data file became available, it was copied to the TIER2 worker node. The data were then searched for periodic signals following the standard search procedures outlined in Manchester et al. (2001) and Lorimer & Kramer (2005): Firstly, the 96 channels were dedispersed to four frequency sub-bands at each value of trial dispersion measure (DM). Just prior to dedispersion the harmful effects of radio frequency interference (RFI) were reduced by application of the zero-DM filter (Eatough et al. 2009). These sub-band data were stored for folding and optimisation of the candidates generated from the acceleration search. The subbands were then dedispersed (without re-application of the zero-DM filter) to a single channel timeseries at the same trial DM. Every four sequential samples in this time series were then summed together, to give a 1 ms sample interval before performing the coherent acceleration search as outlined in Section 3. Features above a pre-defined threshold S/N (calculated from the expected false-alarm probability) in the resulting fluctuation spectra were stored in a candidate list along with the associated DM and acceleration. At this point 'reconstructed S/Ns' were also computed and stored[7]. Harmonic summation of two, four, eight and 16 harmonics was performed to provide sensitivity to narrow pulses (Taylor & Huguenin 1969). The threshold S/N was reduced in successive harmonic folds as the probability density function of spectral features evolves from a Rayleigh to a Gaussian distribution. The whole process was repeated for each trial value of DM and acceleration.

[3] http://www.hep.man.ac.uk/computing/tier2
[4] http://www.gridpp.ac.uk
[5] http://lcg.web.cern.ch/LCG/
[6] http://sigproc.sourceforge.net/
[7] Reconstructed S/N is the S/N of a pulse profile generated from the inverse Fourier transform of the complex frequency components of a signal (e.g. Appendix C, Faulkner 2004, Lorimer & Kramer 2005).

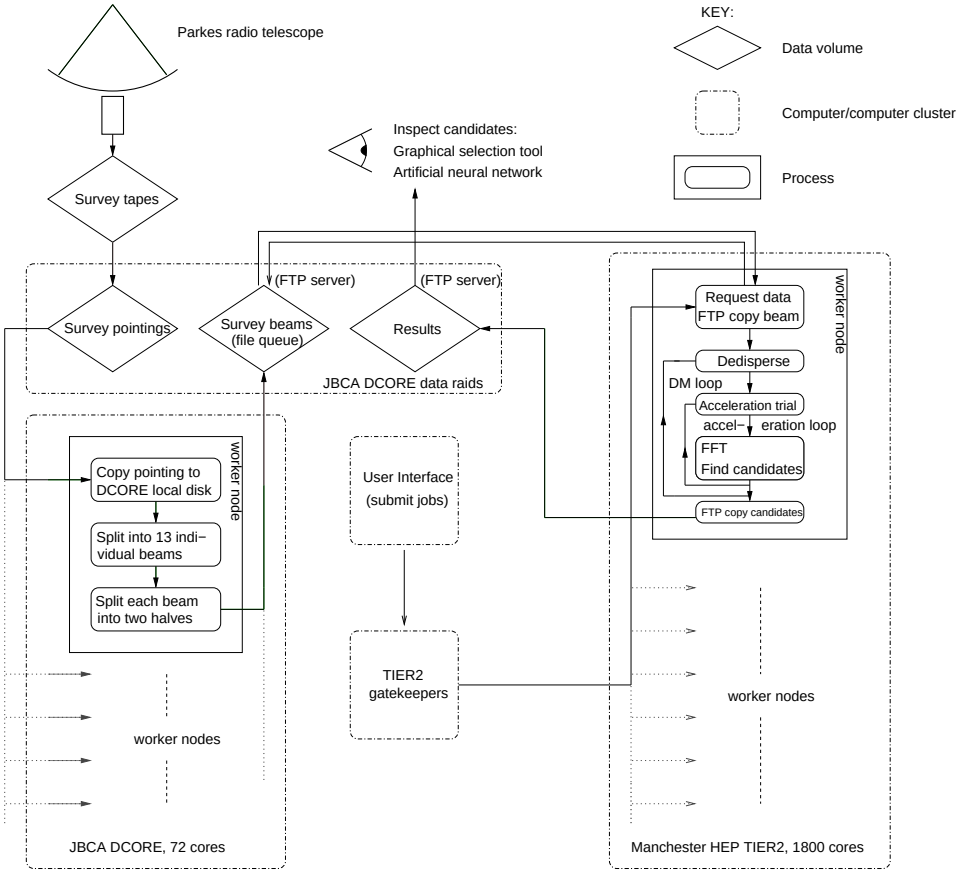

Figure 5. Flow diagram summarizing the PMACCN data processing using the TIER2 facility. The survey pointings were stored on an archive RAID at the Jodrell Bank Centre for Astrophysics (JBCA). Each pointing was separated into 26 half integrations using the DCORE cluster and stored for processing. Jobs were submitted to the TIER2 facility via the 'user interface', a desktop machine at the JBCA. Once a processing job started on a worker node a request for data was made to a control program running on the JBCA RAID host computer. Available files were then copied and processed on the worker nodes. The candidates from the search were sent back to the DCORE cluster where they are viewed with either a graphical selection tool or an artificial neural network (Eatough et al. 2010).

After dispersion and acceleration searching was complete the candidate list was checked for the most significant signals (sorted by their reconstructed S/N) at each DM and acceleration. The DM and acceleration for which each signal was strongest was noted and any harmonics of the signal were checked for and ignored if identified. Signals down to a threshold S/N $\sim$ 9, from each of the 1050 s segments, were stored in a final candidate list. Candidates in this list were then 'optimised' in the time domain using the PULSARHUNTER software package[8]. The appropriate sub-band data file was divided into 64 temporal sub-integrations after which searches over narrow ranges in period, DM and acceleration were performed to find the best integrated pulse S/N. The results of this search and the initial acceleration search were placed into 'candidate plots' for viewing. An example of one such candidate plot, covering the position of PSR J1141−6545, is visible in Figure 6. Finally, all results were compressed with GZIP and returned to the JBCA for inspection.

4.2 Post-processing overview

The total number of pulsar candidates produced by reprocessing the PMPS with the PMACCN search algorithm was in the region of 16 million; a number far in excess of previous analyses. As first noted by Faulkner et al. (2004), such large numbers of pulsar candidates can, in practice, only be inspected with the aid of a graphical selection tool. For this purpose the graphical selection tool JREAPER (Keith et al. 2009) was employed. Despite the advanced filtering techniques that can be performed with JREAPER the number of candidates requiring visual inspection still remained large. As such, an automatic candidate inspection technique, utilising an artificial neural network (ANN), was developed to complement the manual searches performed with JREAPER (Eatough et al. 2010).

Promising pulsar candidates selected with either JREAPER or by the ANN were placed into three categories for follow-up observation: class one, for candidates that had a large probability of being new pulsar discoveries, class three for candidates that had a smaller chance of being new pulsars, and class two, for candidates that were in between the former categories. The majority of candidates viewed were

[8] http://sourceforge.net/projects/pulsarhunter/

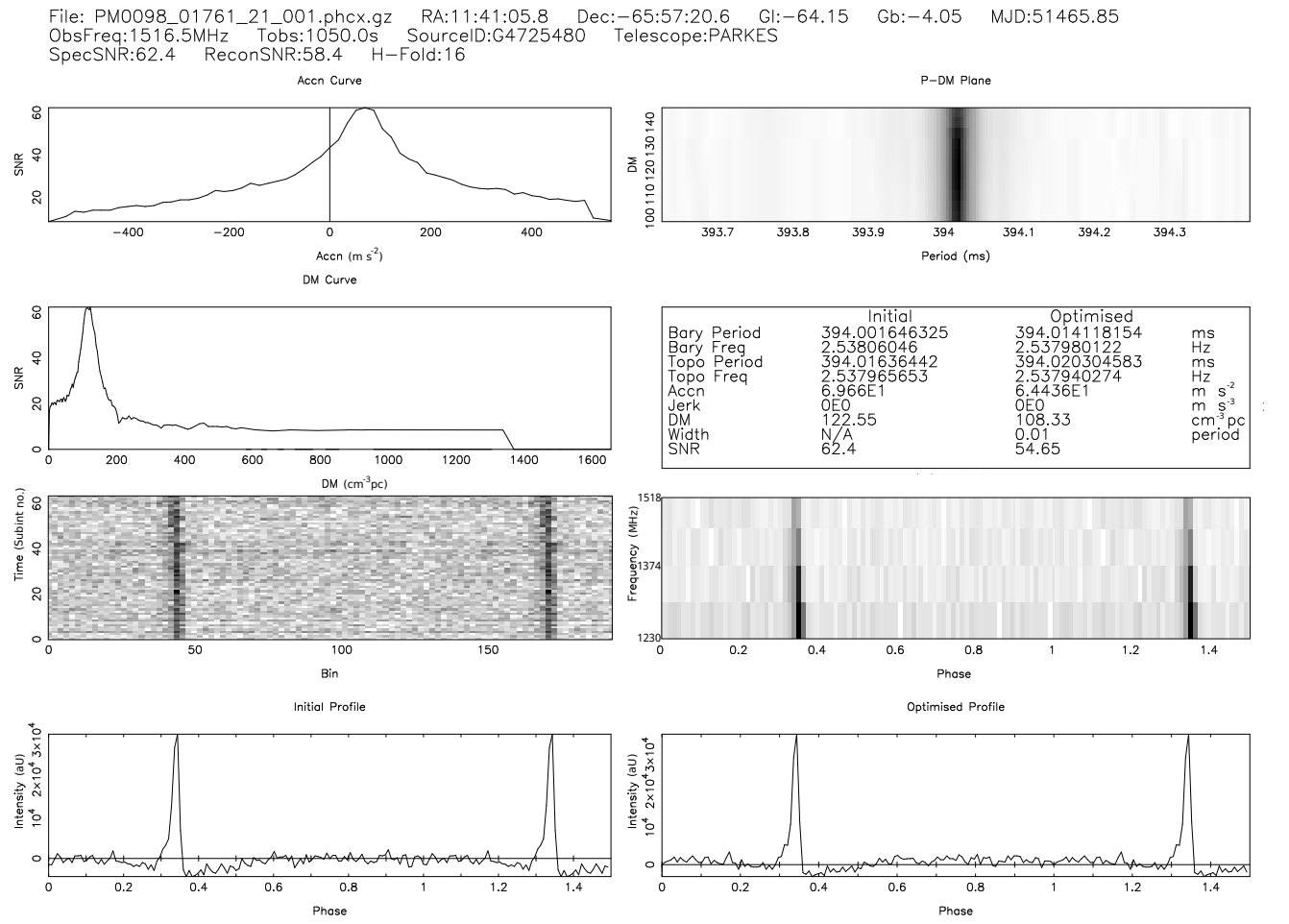

Figure 6. Example candidate plot from the PMACCN algorithm generated for visual inspection of the quality of pulsar candidates and showing a detection the relativistic binary pulsar, J1141−6545. Starting clockwise from the bottom left the candidate plot displays: the integrated pulse profile, folded at the initial spectral discovery period and dispersion measure (DM); 64 temporal subintegrations of the observation, showing how the pulse varies with time; the spectral S/N as a function of a wide range of trial DMs (the DM-S/N curve); the spectral S/N as a function of trial acceleration (the acceleration-S/N curve: here the pulsar has been detected with an acceleration of 64.4 ms^{-2}); the period-DM diagram, that shows how the S/N varies with small changes in the folding period and DM; the basic discovery parameters before and after time domain optimisation; stacked pulses across four frequency subbands, showing how the pulse varies with observing frequency, and finally the integrated pulse profile, folded at the optimum period and dispersion measure. The dips, visible at the edges of the integrated pulse, are caused by application of the zero-DM filter (Eatough et al. 2009).

non-pulsar signals caused by either RFI or noise fluctuations. These signals were discounted.

5 DISCOVERY AND TIMING OF 16 PULSARS

Reprocessing of the PMPS with the PMACCN algorithm has yielded 16 new pulsar discoveries. Despite the improved acceleration search algorithm used in this analysis, no previously unknown relativistic binary pulsars have been found. However, all known relativistic binary pulsars in the survey region have been re-detected with a higher significance than obtained in previous analyses. A number of promising binary candidates have been identified, but to date none have been re-detected despite follow-up observations (see Section 6.2).

Not all of the pulsars found in this work have been detected here for the first time. During comparison of the candidates generated from this search with those from the previous Faulkner et al. (2004) analysis, it was noticed that a number of the previous class one candidates had never been re-observed. These oversights were undoubtedly due to the large number of genuine pulsar discoveries making tracking of the status of each candidate a difficult task. As part of this work, confirmation observations of these sources were performed after which they were added to timing programmes at either the Parkes or Jodrell Bank Observatories. All the pulsars have been timed for a period long enough to determine an accurate position and to derive the basic pulsar parameters. All timing measurements were performed with the PSRTIME software[9].

Table 2 presents the pulsar name, the J2000 right ascension and declination from the timing solution, the Galactic coordinates, the S/N of the discovery observation af-

[9] http://www.jb.man.ac.uk/∼pulsar/observing/progs/psrtime.html

ter the time-domain folding and optimisation, the candidate selection tool by which the pulsar was discovered, the mean flux density at ∼1.4 GHz from the survey detection, S_{1400}, and the pulse width at 50 per cent of the peak of the mean pulse profile, W_{50}. Uncertainties on the values presented, where relevant, are given in parentheses and refer to the last digit. Flux densities have been corrected for positional offsets in the survey detection. Sources marked with a * were not detected in this analysis but were found by reobservation of the unconfirmed class one candidates from the previous Faulkner et al. (2004) reprocessing. Sources marked with a ♣ were detected both in this analysis and the previous analysis but only confirmed now. Sources with no markings have been detected here for the first time. In summary, five of the pulsars were not detected in this reprocessing, three were detected in both, and seven have been newly discovered. The discoveries of PSRs J1539−4828, J1819−1717, and J1835−0114 have already been mentioned in Eatough et al. (2009) and the discovery of PSR J1926+0737, using an ANN, is described in Eatough et al. (2010).

Table 3 gives barycentric pulse periods, period derivatives, epoch of the period, the number of pulse time of arrival (TOA) measurements in the timing solution, the MJD range of the timing observations, the final rms residuals of the timing model, and the dispersion measure. Table 4 gives the following derived parameters of the 16 pulsars: characteristic age, τ_c, surface magnetic field, B_s, rate of loss of rotational energy, $\dot{E}$, the dispersion derived distance using the NE2001 electron density distribution model (Cordes & Lazio 2002), the corresponding height above the Galactic plane, z, and finally the inferred luminosity at 1400 MHz, L_{1400}. High S/N mean pulse profiles of each of the 16 pulsars at 1374 MHz are presented in Figure 7.

Excluding the pulsars that did not appear in this processing (i.e. sources marked with *), the remaining sample exhibits a wide range in flux densities. The discovery of PSR J1716−4005, a source with a large flux density that was completely undetected in previous analyses, has most likely been enabled by effective removal of RFI, by use of the zero-DM filter, and improved candidate selection tools. A number of the sources are below the limiting flux density of our search ($S_{1400} \sim 0.2$ mJy for the centre of the central beam) which is estimated to be of order $\sqrt{2}$ times less sensitive than that in the original searches of the PMPS because of the use of half length, 1050 s integrations. The zero-DM filter may account for this as its use can improve the limiting survey sensitivity by the effective removal of RFI (Eatough et al. 2009). In general the pulsars are consistent with the sample of pulsars found by the PMPS as a whole viz. low flux density but high luminosity because the pulsars are found at relatively large distances. PSR J1818−1448 has a the largest period derivative of the pulsars discovered implying an age of just 720 kyr and making it the youngest of the new sources. Unfortunately, this age is too great to expect any supernova remnant association to be visible.

5.1 Notable discoveries

5.1.1 PSR J1835−0114, a binary millisecond pulsar

Soon after the discovery of PSR J1835−0114, it was noticed that the spin period was not constant but changing periodically. As no sign of period variation was measured in the search output, i.e. over 1050 s integration, the behaviour was thought to be typical of that of a pulsar in a long orbital period binary system. Continued timing observations at Jodrell Bank Observatory have shown that the pulsar is in a 6.7-day orbit, probably around a low mass companion. The measured binary parameters of this system are given in Table 5. The pulsar is in a circular orbit ($e \sim 1 \times 10^{-5}$), typical of pulsars in binary systems that have undergone a long period of accretion powered spin up (Phinney 1992). In non-relativistic systems estimation of the mass of the pulsar and companion, m_p and m_c, can only be made through accurate measurements of the mass function given by

$$f(m_p, m_c, i) = \frac{(m_c \sin i)^3}{(m_p + m_c)^2} = \frac{4\pi^2}{G}\frac{a^3 \sin^3 i}{P_b^2} = 0.00241709 M_\odot, \quad (4)$$

where a is the semi-major axis of the orbit, i is the inclination angle and the other terms have their usual meanings. In order to estimate the mass of the companion a typical neutron star mass of 1.35 $M_\odot$, from the known neutron star masses measured in relativistic binaries (Thorsett & Chakrabaty 1999), has been assumed. Random orbital axis orientation arguments allow us to assume a median inclination angle of 60°, see e.g. Lyne & Smith (2006), page 127. With the observed value of the mass function, an iterative solution for m_c in Equation 4 gives a most likely companion mass of 0.21 $M_\odot$; indicative of a white dwarf star.

5.1.2 PSR J1808-1517, an intermittent pulsar

PSR J1808−1517 was a class one candidate that was detected in only one half of the original 35 minute observation. Analysis of the full integration, revealed the pulsed signal disappearing approximately half way through the observation (see Figure 8 top panel). The candidate class, combined with observed parameters typical of normal pulsars ($P \sim 544$ ms, DM ~ 205 cm^{-3}pc, pulse duty cycle ∼4 per cent) pointed to a clear pulsar detection. However, in approximately seven hours of follow up observations performed on different dates at the Parkes observatory and regular observations from March 13th to September 9th, 2008 at the Jodrell Bank observatory, no re-detection was made. Despite the expected difficulty in confirmation it was decided to continue with observations at the Parkes observatory at approximately monthly intervals. In March 2010 a re-detection was made. To confirm the intermittent nature of this pulsar, reobservations were performed at the Effelsberg observatory. The bottom panel of Figure 8 shows temporal subintegrations over a 31 minute observation done at Effelsberg. During this observation the pulsar exhibits nulls lasting the order of a few minutes, with a nulling fraction of ∼ 50 per cent. Because of the earlier non-detections, we suggest the length of nulls vary and could be at least as long as a typical observation time ($\gtrsim 30$ minutes). Based on the Effelsberg observation the switching time scale between states is $\lesssim 12$ s ($\lesssim 23$ pulse periods).

Table 2. Positions, survey beam in which the pulsar was discovered, candidate selection tool used in the discovery, folded S/N, flux densities and pulse widths of the 16 pulsars discovered in this work. Positional uncertainties are derived from the one-sigma error of the timing model fit obtained using the PSRTIME software. See Section 5. for an explanation of the symbols.

PSR J	R.A. (J2000) (h min s)	Dec. (J2000) (° ′ ″)	l (°)	b (°)	S/N	Selection tool	S_{1400} (mJy)	W_{50} (ms)
J1539−4828	15:39:40.84(6)	−48:28:57(1)	329.43	+5.54	9.5	JREAPER	0.20(2)	50.9
J1638−3951*	16:38:15.56(5)	−39:51:59(1)	343.00	+4.74	10.2	n/a	0.21(2)	61.7
J1644−4657*	16:44:38.5(1)	−46:57:38(4)	338.43	−0.81	8.9	n/a	0.59(5)	40.3
J1655−3844*	16:55:38.66(5)	−38:44:09(1)	346.04	+2.91	10.9	n/a	0.25(2)	95.5
J1701−4958♣	17:01:12.83(6)	−49:58:33(2)	337.84	−4.84	11.2	JREAPER	0.26(1)	128.7
J1716−4005	17:16:42.06(4)	−40:05:27(2)	347.42	−1.15	56.2	JREAPER	1.37(1)	48.9
J1723−2852	17:23:58.2(3)	−28:52:51(15)	357.47	+4.01	10.6	JREAPER	0.13(1)	50.0
J1808−1517	18:08:39.09(2)	−15:17:40(2)	14.47	+2.24	12.5	JREAPER	0.35(3)	21.8
J1818−1448*	18:18:27.91(6)	−14:48:38(7)	16.03	+0.39	9.7	n/a	0.19(1)	45.0
J1819−1114♣	18:19:28.78(1)	−11:14:43(1)	19.29	+1.86	13.7	JREAPER	1.07(5)	94.1
J1819−1717	18:19:43.40(5)	−17:17:16(5)	13.99	−1.05	11.3	JREAPER	0.26(2)	31.5
J1835−0114	18:35:21.9179(9)	−01:14:33.61(2)	29.99	+3.01	11.8	JREAPER	0.10(1)	0.2
J1840−0753	18:40:47.6(1)	−07:53:32(6)	24.70	−1.24	13.1	JREAPER	0.37(2)	140.1
J1845−0635♣	18:45:07.406(9)	−06:35:23.4(8)	26.35	−1.60	31.0	JREAPER	0.36(1)	27.2
J1854+0317*	18:54:29.06(7)	+03:17:31(3)	36.21	+0.82	10.5	n/a	0.12(1)	109.3
J1926+0737	19:26:33.740(6)	+07:37:07.2(3)	43.74	−4.26	10.2	ANN	0.11(1)	25.4

Table 3. Timing parameters and dispersion measures of the 16 pulsars discovered in this work. Spin period uncertainties are derived from the one-sigma error of the timing model fit obtained using the PSRTIME software. See Section 5. for an explanation of the symbols.

PSR J	Period, P (s)	$\dot{P}$ (10^{-15})	Epoch (MJD)	$N_{\rm toa}$	Data span MJD	Residual μs	DM cm^{-3}pc
J1539−4828	1.27284159978(14)	1.267(2)	54845.0	22	54647−55043	1590	117(5)
J1638−3951*	0.77113024025(8)	0.59(4)	54863.3	22	54683−55043	1014	249(4)
J1644−4657*	0.12596223249(4)	0.75(2)	54835.1	16	54683−54988	1792	718(6)
J1655−3844*	1.19343919921(14)	2.00(6)	54863.3	22	54683−55043	1144	365(11)
J1701−4958♣	0.80430423739(12)	0.11(4)	54844.6	25	54646−55043	2332	230(5)
J1716−4005	0.31181276456(4)	2.87(4)	54942.8	15	54842−55043	160	435(3)
J1723−2852	0.6250339127(12)	0.9(16)	54948.6	31	54862−55691	1895	172(6)
J1808−1517	0.544549207067(8)	2.6671(5)	55105.4	94	54596−55615	1035	205(5)
J1818−1448*	0.28137130037(6)	6.15(2)	54863.1	28	54683−55043	3142	644(6)
J1819−1114♣	0.29416251457(2)	0.566(6)	54849.9	81	54652−55048	1222	310(5)
J1819−1717	0.39352163764(6)	3.455(6)	54756.2	75	54529−54983	1698	405(2)
J1835−0114	0.005116387644239(12)	0.000007(4)	54786.8	142	54540−56010	107	98(1)
J1840−0753	0.4378690017(2)	0.10(6)	54803.9	140	54559−55049	20061	691(7)
J1845−0635♣	0.34052764699(2)	4.491(8)	54844.5	65	54656−55033	744	414(1)
J1854+0317*	1.3664496471(2)	1.85(16)	54863.5	18	54683−55043	2472	404(8)
J1926+0737	0.318062050971(12)	0.375(4)	54833.6	48	54619−55048	704	159(2)

This analysis of the PMPS, that has searched independent halves of the original 35 minute integrations, has aided in the detection of this pulsar. The addition of the second half of the original observation, when the pulsar was not visible, reduces the integrated pulse S/N down to 8.5 and places the pulsar on the limit of previous detection thresholds.

5.1.3 J1926+0737, a pulsar with an interpulse

PSR J1926+0737, that was found using an ANN (Eatough et al. 2010), exhibits an interpulse at a rotational phase $\sim 180^\circ$ from the main pulse. This characteristic implies that the angle between the magnetic axis and the

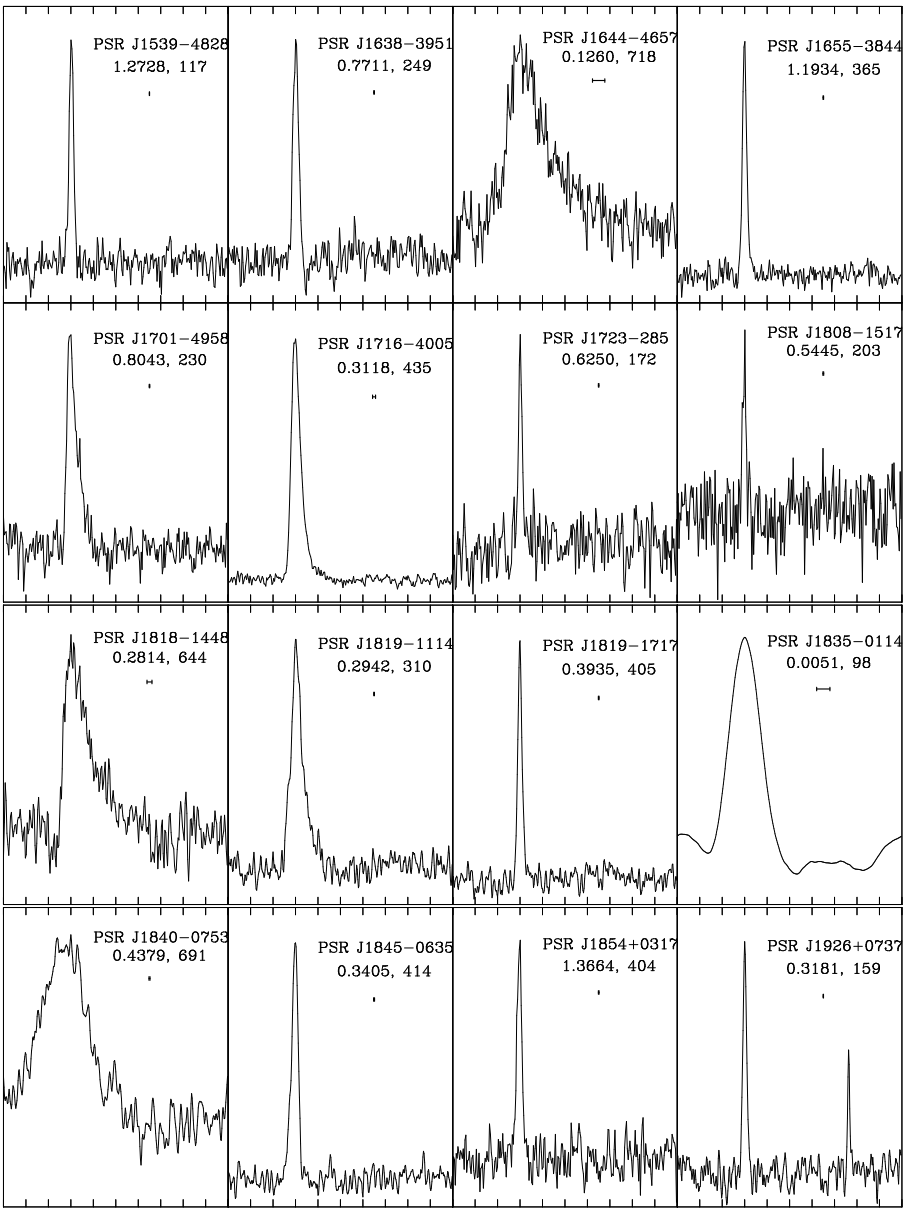

Figure 7. Mean pulse profiles over a phase of zero to one at 1.4 GHz for the 16 pulsars. The peak of each profile has been centered at a phase of 0.3. Each panel also displays the pulsar name, pulse period in seconds, and dispersion measure in $\mathrm{cm}^{-3}\mathrm{pc}$. The effective time resolution of the profile, including the effects of interstellar dispersion, is indicated by the horizontal error bar below the text.

rotational axis, α, is $\sim 90^\circ$ and that the pulsar must be an orthogonal rotator, where emission from both magnetic poles is visible. This pulsar adds to the population of 31 normal pulsars (with $P > 20$ ms) that exhibit interpulses (Maciesiak et al. 2011). The properties of pulsars with interpulses are of importance for understanding the evolution of pulsar beams, which has implications in the long term spin-down behaviour of pulsars and also in the number of pulsars likely to be detected in future pulsar surveys (e.g. Weltevrede & Johnston 2008, Maciesiak et al. 2011).

6 DISCUSSION

In this section we start with a brief comparison of our results with the available predicted number of relativistic binary pulsars in the PMPS (Section 6.1). We then outline some of the possible reasons for the non-detection of new relativistic binary systems (Section 6.2), before describing further tests of the acceleration algorithm used here (Section 6.3). Lastly, Section 6.4 is a brief discussion of the promising pulsar candidates detected with PMACCN, but which have never been confirmed in re-observations.

Table 4. Derived parameters of the 16 pulsars discovered in this work. Distances have been calculated based on the Cordes & Lazio (2002) free electron density model of the Galaxy. See Section 5 for an explanation of the symbols.

PSR J	τ_c (Myrs)	$\log B_s$ (G)	$\log \dot{E}$ (erg s^{-1})	Distance (kpc)	z (kpc)	L_{1400} (mJy kpc^2)
J1539−4828	15.96	12.10	31.38	3.6	+0.35	1.3
J1638−3951*	20.65	11.83	31.71	5.4	+0.45	3.2
J1644−4657*	2.65	11.49	34.17	8.2	−0.12	14.8
J1655−3844*	9.43	12.19	31.67	6.5	+0.33	5.1
J1701−4958♣	115.53	11.47	30.92	4.9	−0.41	5.8
J1716−4005	1.72	11.98	33.57	5.4	−0.11	33.0
J1723−2852	10.97	11.88	32.16	3.4	+0.24	1.4
J1808−1517	3.23	12.08	32.81	3.8	+0.15	1.6
J1818−1448*	0.72	12.12	34.04	7.4	+0.05	8.2
J1819−1114♣	8.21	11.61	32.94	5.0	+0.16	9.8
J1819−1717	1.80	12.07	33.35	5.6	−0.10	5.3
J1835−0114	11548.42	8.28	33.31	2.7	+0.14	0.7
J1840−0753	69.18	11.32	31.67	10.0	−0.22	30.0
J1845−0635♣	1.20	12.09	33.65	7.1	−0.20	17.6
J1854+0317*	11.67	12.20	31.46	7.5	+0.11	6.2
J1926+0737	13.40	11.54	32.66	5.6	−0.42	3.1

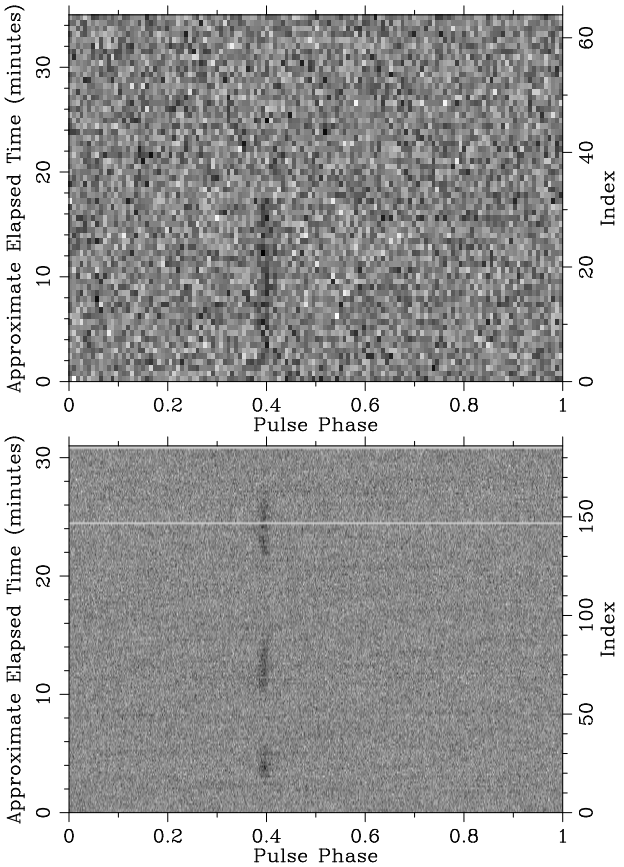

Figure 8. Phase resolved pulse amplitude as a function of time for the original PMPS observation of PSR J1808-1517 (top panel) and a re-observation performed at the Effelsberg observatory (bottom panel). Subintegrations are plotted every $\sim$ 30 s and $\sim$ 12 s for the PMPS and Effelsberg observations respectively.

Table 5. Binary parameters of PSR J1835−0114. Uncertainties on the values presented are given in parentheses and refer to the last digit.

Parameter	Value
Orbital period (days)	6.6925427(4)
Projected semimajor axis $x = (a/c)\sin i$ (s)	4.654423(7)
Orbital eccentricity e ($\times 10^{-5}$)	1.1(3)
Longitude of periastron ω (°)	-3(1)
Epoch of periastron (MJD)	54540.7(3)
Mass function ($M_\odot$)	0.00241709(4)

6.1 Comparison of results to binary population predictions

To date, this acceleration search of the PMPS has not increased the number of relativistic binary systems discovered in the survey. Prior to the commencement of this work, and using a method based on the observed sample of DNS systems (Kim et al. 2003), Kalogera et al. (2004) made a prediction that approximately another 4 ± 2 (error estimated from Figure 2. of Kalogera et al. (2004)) compact binary pulsars (with properties similar to either PSRs B1913+16, B1534+12, and J0737−3039A/B) remained to be discovered in the PMPS data, and would be detectable with effective acceleration searches. The Faulkner et al. (2004) re-analysis of the PMPS proved that there were indeed binary systems that had previously been missed because acceleration searches were not used, including one compact DNS system, PSR J1756−2251. PSR J1906+0746 was also detected with high significance in this analysis but missed at the candidate selection stage (Lorimer et al. 2006). Currently PSR J1906+0746 is believed to be a young pulsar with a heavy

white dwarf companion, so does not belong to the category of systems described by Kalogera et al. (2004). The number of relativistic DNS systems discovered in the PMPS is therefore less than the Kalogera et al. (2004) prediction. If PSR J1906+0746 is in fact a DNS system, the current number of compact DNS in the PMPS would be two; still less than predicted. Whatever the nature of the companion, the youth of PSR J1906+0746 implies that the underlying population of this type of system could be larger (Lorimer et al. 2006).

Alternative Galactic population predictions, from binary synthesis methods, differ by orders of magnitude in the number of DNS and NS-BH systems produced because of large uncertainties in the model parameters used to describe key stages of binary evolution; such as the magnitude of supernova kicks and the outcome of common envelope evolution (see e.g. Bethe & Brown 1998, Portegies Zwart & Yungelson 1998, Nelemans et al. 2001, Sipior & Sigurdsson 2002, Belczynski et al. 2002, Voss & Tauris 2002, Sipior et al. 2004, Lipunov et al. 2005, Pfahl et al. 2005, Belczynski et al. 2010, Osłowski et al. 2011). The population constraints provided by the binary pulsar search analysis performed here, and similar binary searches, can be used to improve and calibrate binary population synthesis codes. However, the result of a non-detection should be treated with caution due to a number of selection effects and stages at which pulsar candidates can easily be lost. Some of these points are discussed in the following section.

6.2 Possible reasons for the non-detection of new relativistic binaries

Although this search can help to constrain the numbers of new relativistic binary pulsar systems, our non-detection does not necessarily imply that there are no more of these systems to be found. A more likely scenario is that these pulsars have been missed because of any one of a number possible reasons, some of which are listed below. For example, such pulsar systems might be

- below the limiting sensitivity of the PMPS. For this search of 1050 s segments, the best sensitivity of ~ 0.2 mJy is achieved in the centre of the central beam.
- at an orbital phase where the acceleration was not constant (see Section 6.3.1).
- outside the range of orbital accelerations searched (see Section 6.3.2).
- undetected because they are in a survey beam with excessive RFI. Despite the use of the zero-DM filter, which reduces the amount of the fluctuation spectrum that is removed to virtually zero (Eatough et al. 2009), RFI can reduce the sensitivity of the survey. Unfortunately it is difficult to quantify this effect (Manchester et al. 2001).
- detected but not found during candidate selection (see e.g. Keith et al. 2009, Eatough et al. 2010). Pulsar surveys produce many millions of pulsar candidates which are typically inspected by eye and which can lead to promising candidates being overlooked. The missed discovery of PSR J1906+0746 in the PMPS illustrates this (Lorimer et al. 2006). Attempts in this work were made to automate this process using an ANN (see Section 4.2 and Eatough et al. 2010).
- already detected but cannot be confirmed with follow-up observations either because of intermittent emission (see e.g. Section 5.1.2) or because the emission beam has precessed out of the line-of-sight (see Section 6.4).
- undetected as they were not emitting during the survey observation because they are a different class of pulsar, e.g. Rotating Radio Transients (McLaughlin et al. 2006) or intermittent pulsars (Kramer et al. 2006).
- not in the region of sky covered by PMPS. See below for details of the new all-sky pulsar surveys.

As already mentioned, some of these points are un-avoidable and others cannot be addressed until new more sensitive pulsar surveys, such as the all-sky High Time Resolution Universe (HTRU) surveys (Keith et al. 2010, Barr et al. in prep) are fully searched for binaries (Ng 2011, Ng et al. in prep), or until surveys to be performed with the next generation of radio telescopes, e.g. LOFAR, FAST, and the SKA (e.g. Stappers et al. 2011, van Leeuwen & Stappers 2010, Smits et al., 2009a,b, Cordes et al., 2004) are completed. Some of the other points, relevant to this analysis, are now discussed in more detail.

6.3 Additional acceleration search algorithm tests

After the previous re-processing of the PMPS (Faulkner 2004, Faulkner et al. 2004) it was understood that much of the sensitivity of the survey to relativistic binary pulsars was being lost because of two principal effects: firstly, the incoherent addition of spectra in the stack acceleration search and secondly, no compensation for the effects of jerk caused by large changes in orbital phase throughout the 35 minute observations. These problems have been partially addressed in this work by implementing a coherent acceleration search over a wide range of trial accelerations, and upon independent halves of the original 35 minute integrations. To establish if any systematics in the PMACCN algorithm were responsible for the non-detection of any new relativistic binary pulsars we have performed a number of additional tests, which are described in this section. Because the primary goal of this work has been to find relativistic binary systems like the Double Pulsar (and those more extreme binary systems) we have chosen this system as our test case.

6.3.1 Integration length analysed and orbital phase effects

Since the acceleration search technique can only correct for the quadratic drift in pulse phase (and the corresponding linear drift in pulse frequency) caused by a constant acceleration, sensitivity would have been lost to any systems that showed changes in acceleration during the PMPS observation. Without performing the higher order corrections necessary to remove the effects of jerk, the only method by which this can be mitigated in an acceleration search is to reduce the integration length analysed (Johnston & Kulkarni 1991). In addition, the orbital phase at which the pulsar is observed will determine how well the constant acceleration assumption can model the data. To study both the effects of the integration length analysed (to find if the 1050 s integration time used in this work was optimal for the detection of relativistic binary systems), and

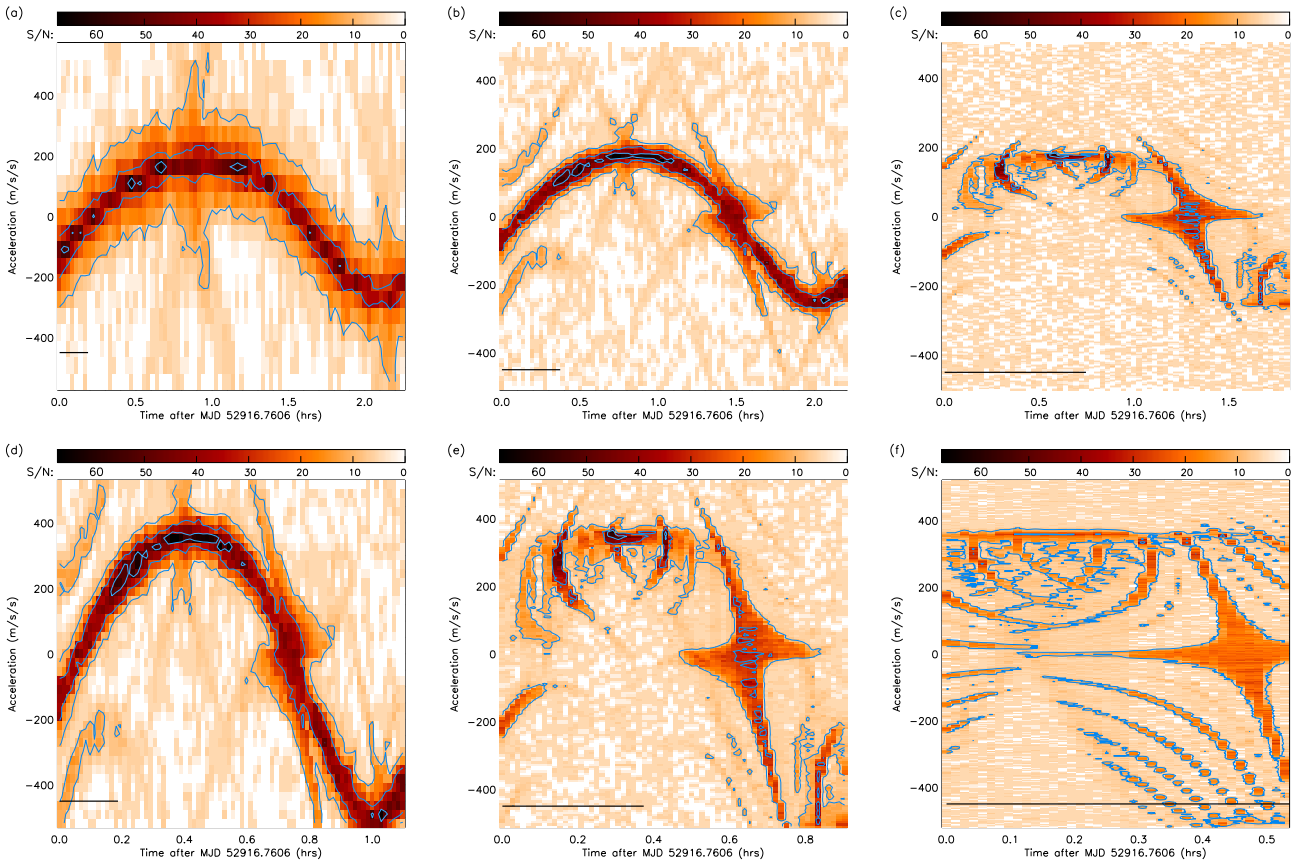

Figure 9. The results from acceleration searches, using different integration lengths, across a 2.6 hour Parkes observation of the Double Pulsar system (panels (a), (b), and (c)) and the same data, but modified with a false sampling interval half that of the original to effect a 1.2 hour binary (panels (d), (e), and (f)). Each panel shows the spectral S/N (of PSR J0737−3039A) as a function of trial acceleration for acceleration searches incremented in orbital phase by 100 seconds (panels (a), (b), and (c)) and 50 seconds (panels (d), (e), and (f)). The left-hand column of panels (panels (a) and (d)) show acceleration searches performed with an integration length of 671 seconds, the middle column (panels (b) and (e)) 1342 seconds, and the right-hand column (panels (c) and (f)) 2684 seconds. The black bar at the bottom of each panel indicates the length of the integration time used in each acceleration search. The maximum and average S/N_{peak} are summarized in Table A1 and are given here as follows. Panel (a): 62.6, 43.7, panel (b): 66.9, 48.3, panel (c): 62.8, 32.4, panel (d): 66.6, 48.3, panel (e), 62.8, 32.4, panel (f): 36.4, 29.1. Contours, plotted on top of the colour scale, mark spectral S/Ns of 10, 30, and 60.

to probe the effects of orbital phase at which the pulsar is observed, the following tests have been performed: Acceleration searches using different integration lengths, and separated by short intervals in orbital phase, have been performed on archival data, from the Parkes radio telescope, that covers one full orbit of the Double Pulsar system. Additionally, to create a more rigorous test, the same data have been modified with a false sampling interval half that of the original 80 μs. This has the effect of halving both the pulse and orbital period, and doubling the apparent line-of-sight acceleration to $\sim 520\,\mathrm{m\,s^{-2}}$.

Three integration times, that are similar to small factors of the original PMPS integration time, have been investigated: "full-length" 2684 second segments, "half-length" 1342 second segments, and "quarter-length" 671 second segments[10]. Appropriate step sizes in acceleration trail for each integration length have been computed using Equation 3. To investigate the effects of orbital phase on the different length acceleration searches, the starting point of each search has been incremented by 100 seconds for the original data, and 50 seconds for the modified data across the entire orbit.

In Figure 9 the results of these tests are presented. Each panel shows the spectral S/N of PSR J0737−3039A as a function of trial acceleration for an acceleration search started at a time after MJD 52916.76 given in hours. Figure 9 panels (a), (b) and (c) show the results from the original, un-modified data. Results from these tests are also summarized in Table 6 in addition to results from tests accounting for the effects of jerk (Section 6.3.3). Acceleration searches of the quarter and half-length segments (panels (a) and (b) respectively) are comparable in their sensitivity over all orbital phases although there is a small improvement in sensitivity for the half-length segments, which show both a higher maximum and average peak spectral

[10] The integration times investigated do not match exact factors of the original PMPS observation time because of the use of a different data sampling interval, and a technical requirement in the tests for a total number of samples equal to a power of two.

S/N (S/N_{peak}) across the orbit[11]. Importantly, the average S/N_{peak} in the half-length segments is larger only by a factor of ~ 1.1 compared to the quarter-length segments; less than the expected increase of $\sqrt{2}$ given by the radiometer equation. This can be explained by a reduction in sensitivity in the half-length segments because of the increased effects of jerk. This deleterious effect is confirmed by the fact that the maxima in S/N_{peak} occur at integrations that cover orbital phases where the acceleration is closest to constant, viz. at the peaks and troughs. The corresponding minima in S/N_{peak} occur at orbital phases where the acceleration is changing most rapidly. In the quarter-length analysis (panel (a)), where the acceleration can be considered constant at almost all orbital phases, the maxima in S/N_{peak} occur more evenly across the orbit.

As expected, the effectiveness of acceleration analyses using the full-length segments (panel (c)), is strongly dependent upon orbital phase. Although a maximum S/N_{peak}, comparable to those in the shorter analyses, can be achieved, the average S/N_{peak} is significantly reduced by a factor of ~ 1.5 with respect to half-length analyses.

Figure 9 panels (d), (e), and (f) show the results from acceleration searches of the data modified with a false sampling interval and using the same integration length segments as previously. In this data, where the effective orbital period is now 1.2 hours, only acceleration searches that are performed on the short quarter-length segments (panel (d)) have sensitivity across all of the orbit. Both the values of the maximum and average S/N_{peak} in this search (66.6 and 48.3 respectively) and the occurrence of maxima in S/N_{peak} at orbital phases where the acceleration is changing slowly (peaks and troughs) make this the direct analogue of the half-length analysis of the un-modified data (panel (b)), but with an acceleration range expanded by a factor of two. The same situation applies to panels (c) and (e). Therefore, an analysis based on 336 s integrations on the modified data should repeat the results of the 671 s analysis of the un-modified data (panel (a)). Tests using full-length integrations on the modified data produce the lowest values of maximum and average S/N_{peak} from all the tests performed. Because of the relative brightness of PSR J0737−3039A, detections can still be made at most orbital phases, however compared to the optimum acceleration search of the modified data (671 s segments) the average S/N_{peak} is reduced by 40 per cent.

From these tests it is clear that the effectiveness of acceleration searches for the detection of 'Double Pulsar like' systems in long integration lengths ($T_{obs} \gtrsim 2000$ s) are highly dependent upon the orbital phase at which the pulsar is observed. With the integration length used in this work (1050 s) the sensitivity to these systems lies somewhere in between the tests displayed in Figure 9 panels (a) and (b), suggesting this search should be sensitive to such systems at most orbital phases. For systems like the modified Double Pulsar system ($P_b = 1.2$ hrs, maximum acceleration ~ 520 m s^{-2}) the possibility of detection in this work is strongly dependent on the orbital phase at which the pulsar was observed; the search is most effective when the pulsar is maximally accelerated.

[11] S/N_{peak} refers to the best spectral S/N achieved in the acceleration search. The maximum S/N_{peak} is the highest value found in the acceleration searches across the orbit. The average S/N_{peak} is an average of all acceleration searches performed across the orbit.

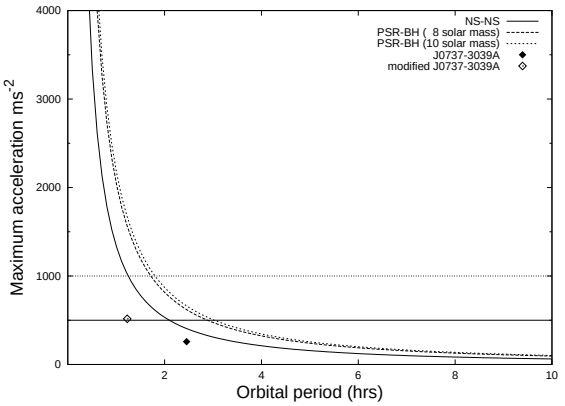

Figure 10. Maximum line-of-sight orbital acceleration as a function of orbital period for circular edge on binary systems. The neutron stars have a mass of 1.3 $M_\odot$ and the two black hole companions have a mass of 8 $M_\odot$ and 10 $M_\odot$. The solid horizontal line shows the magnitude of the maximum constant acceleration that this search was sensitive to of ± 500 m s^{-2}. The diamond points show the maximum acceleration of PSR J0737−3039A in the Double Pulsar system and the "modified" Double Pulsar system described in Section 6.1.1.

6.3.2 Acceleration search range

Neglecting the effects of jerk, and only considering the magnitude of the orbital accelerations that might be present in even more compact DNS and NS-BH systems, it can be shown that the search performed in this work would not be capable of detecting these systems. Figure 10 shows the maximum line-of-sight acceleration as a function of orbital period, for circular edge on binary systems, as given by Kepler's laws. In all curves the neutron stars have a mass of 1.3 $M_\odot$ and the two black hole companions have a mass of 8 $M_\odot$ and 10 $M_\odot$. The solid horizontal line shows the magnitude of the maximum constant acceleration that this search was sensitive to of ± 500 m s^{-2}. The maximum accelerations present in the Double Pulsar system and in the 'modified' Double Pulsar system, described in Section 6.1.1, are indicated by the diamond points.

Using the PMACCN algorithm the most compact circular NS-BH system that might be detectable would in be in an orbit of about three hours. To have an improved chance of finding the most extreme NS-BH systems ($P_b \gtrsim 2$ hr) the acceleration search range should reach at least ± 1000 m s^{-2} (dotted horizontal line). Performing an acceleration search over this range, and with a computational cost no more than that used in the PMACCN algorithm, could be achieved by segmenting the PMPS data into four 525 s segments per beam.

6.3.3 Including jerk

From an extension of the acceleration algorithm presented in Section 3 a step-size in jerk can be computed. The pulse

Table 6. Summary table of results from acceleration and acceleration and jerk searches on the Double Pulsar system (J0737−3039A) and the "modified" Double Pulsar system (J0737−3039A*). S/N_{peak} refers to the best spectral S/N achieved in the acceleration and acceleration and jerk search. The number of acceleration (or acceleration and jerk) trials at each DM searched, n_{trials}/DM, is quoted for a downsampled sampling interval used in each test of 1280 μs for J0737−3039A and 640 μs for J0737−3039A*.

T_{obs} (s)	(acceleration searches)			(acceleration + jerk searches)		
	n_{trials}/DM	Maximum S/N_{peak}	Average S/N_{peak}	n_{trials}/DM	Maximum S/N_{peak}	Average S/N_{peak}
J0737−3039A:						
671	21	62.6	43.7	21	62.6	43.7
1342	75	66.9	48.3	375	66.9	51.9
2684	295	62.8	32.4	7965	84.2	53.8
J0737−3039A*:						
671	21	66.6	48.3	-	-	-
1342	75	62.8	32.4	-	-	-
2684	295	36.4	29.1	-	-	-

broadening due to jerk, τ_{jerk}, can be written,

$$\tau_{jerk}(t) = jt^3/6c, \quad (5)$$

where j is the value of line-of-sight jerk, typically given in units of $cm\,s^{-3}$, t is time and c is the speed of light (see for example Equation 4 in Johnston & Kulkarni 1991). Following the principles outlined in Section 3 the maximum acceptable value of pulse broadening due to jerk at either end of the integration should be $8\tau_{samp}$ for at least 50 per cent of the pulses to be smeared by less than one time sample. A maximum pulse broadening time of $8\tau_{samp}$ allows a step of $16\tau_{samp}$ between jerk trials. Setting Equation 5 equal to this value and once again letting $t = T_{obs}/2$, the step-size in jerk, δj can be written as,

$$\delta j = 768c\tau_{samp}/T_{obs}^3. \quad (6)$$

To find the sensitivity to be gained by correcting for jerk we have re-performed the tests described in Section 6.3.1 on the un-modified Double Pulsar data (Figure 9 panels (a),(b), and (c)). Step sizes have been computed with Equations 3 and 6 and a range in jerk of $\pm 20\ cm\,s^{-3}$ (c.f. jerk in Double Pulsar system $\sim 18\ cm\,s^{-3}$) has been searched. Again, the maximum and average values of S/N_{peak} across the orbit for the different integration lengths are summarized in Table 6. Tests on the 'modified' Double Pulsar system have not been performed due to limitations in available computing power. For the the shortest quarter-length analysis (671 s) the results are the same as the acceleration tests as no jerk trials are required within the range we have chosen. For the half-length segments there is no change in the maximum S/N_{peak} achievable but the average S/N_{peak} has increased by seven per cent. The biggest improvement from the application of jerk corrections is in the full-length (2684 s) segments where both the best maximum and average S/N_{peak} from all of the searches are achieved. These results can also be seen in Figure 11 where the cumulative value of S/N_{peak} of PSR J0737−3039A from the acceleration and acceleration and jerk searches across the Double Pulsar orbit are plotted.

From Table 6 and Figure 11 it can also be seen that the improvement in average S/N_{peak} across the orbit between acceleration and jerk searches of the half-length and full-length integrations is small (factor of 1.04). Because there are a factor of ~ 21 times more trials to perform the acceleration and jerk analyses on the full-length segments compared to the half-length segments, there appears to be large computational expense with little gain in sensitivity. These lower than expected gains in sensitivity by including jerk trials are most likely due to poor approximation of the line-of-sight orbital motion over the length of the integration. To combat these effects a third derivative of velocity might need to be included.

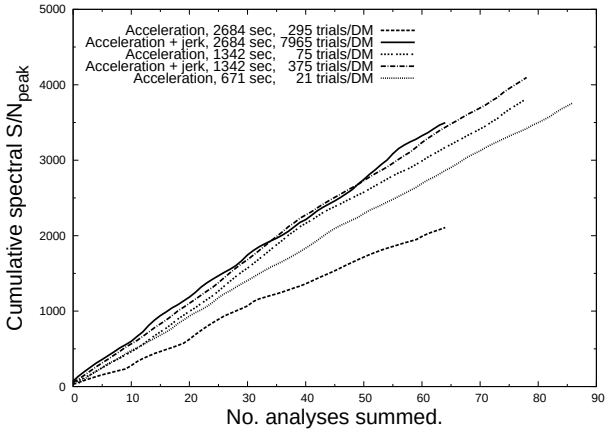

Figure 11. The cumulative S/N_{peak} for detections of PSR J0737−3039A from the acceleration and acceleration and jerk searches across one orbit of the Double Pulsar system.

6.4 Pulsar candidate non-confirmations

Although no relativistic binary systems have been discovered the acceleration search has produced a number of high-quality candidates that have not been confirmed, despite multiple re-observations at either the Parkes or Jodrell Bank observatories. Figure 12 shows an example of one such source, J1431−6042, a highly accelerated class three candidate. This candidate has been followed up with a 'grid' observation (e.g. Morris et al. 2002) and around four hours of re-observations at Parkes. Because the orbital phase and hence the orbital acceleration are likely to be different upon re-observation all the data have been searched in acceleration on the TIER2 facility with the PMACCN algorithm,

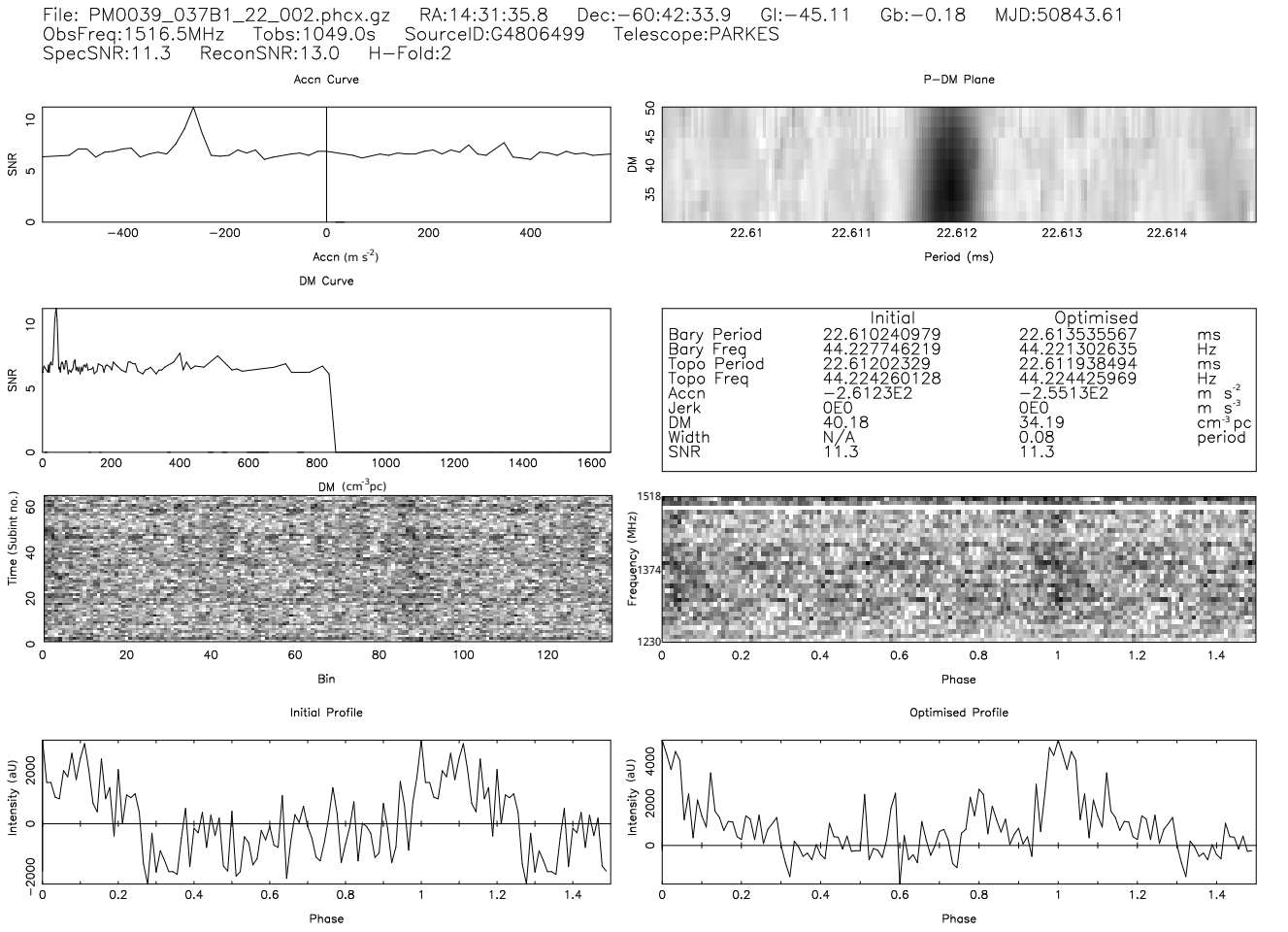

Figure 12. The class three relativistic binary pulsar candidate, J1431−6042. Starting clockwise from the bottom left the candidate plot displays: the integrated pulse profile, folded at the initial spectral discovery period and DM; 64 temporal subintegrations of the observation, showing how the pulse varies with time; the spectral S/N as a function of a wide range of trail DMs; the spectral S/N as a function of trial acceleration (here the pulsar candidate has been detected with an acceleration of -255 ms^{-2}); the period-DM diagram, that shows how the S/N varies with small changes in the folding period and DM; the basic discovery parameters before and after time domain optimisation; stacked pulses across 32 frequency subbands, showing how the pulse varies with observing frequency, and finally the integrated pulse profile, folded at the optimum period and DM.

and independently with the PRESTO software suite[12] over a wider range of accelerations and including corrections for jerk. To date no conclusive re-detection of this candidate has been made.

In total there are 12 other candidates for which a similar situation applies. The majority come from our class two and class three candidate lists. Typically these candidates appear accelerated, have a S/N near our detection threshold (S/N $\sim$ 9), and are often only found in one of the half integrations. Many of these detections might be attributed to strong 'de-accelerated' RFI signals. Strong periodic RFI can appear in the higher DM trials and sometimes even swept in radio frequency mimicking a dispersed signal. In addition, RFI signals are typically unstable causing them to drift through a number of spectral bins in the fluctuation spectrum.

If any of these candidates are in fact true celestial sources the systems may have undergone geodetic precession, where the spin axis of the pulsar precesses with respect to the total angular momentum of the system, which is dominated by the orbital angular momentum (Damour & Ruffini 1974). In a manner similar to that shown for PSR B1913+16 by Kramer (1998), the effect may have shifted the orientation of emission beam away from the Earth over the $\sim$10 years since the original PMPS observation. This is the current explanation for why the relativistic binary pulsar, J1141−6545 (Kaspi et al. 2000) was not detected in an earlier 70 cm survey that covered the position (Manchester et al. 2010). We can estimate the magnitude of geodetic precession for candidates that are close to the orbital period limit of our search. Assuming a minimum detectable orbital period of $\sim$ 3 hrs (using the PMACCN search algorithm) gives a precessional rate of 3.5° yr^{-1} for circular DNS systems (neutron star mass of 1.3 $M_\odot$) and 14.7° yr^{-1} for circular NS-BH systems (black hole mass of 10.0 $M_\odot$). Although the alignment between the spin axis

[12] http://www.cv.nrao.edu/∼sransom/presto/

of the pulsar and orbital angular momentum axis is important in determining by how much the emission beam will move, it is possible that relativistic systems detected in the PMPS survey observations may have precessed out of the line-of-sight in the intervening years.

At the time of writing, observations to detect unconfirmed candidates from this search are still performed when telescope time becomes available.

7 SUMMARY & FUTURE WORK

A full re-analysis of the PMPS has been performed using coherent acceleration searches on independent halves of the original 35 minute integrations. 16 pulsars have been discovered, including a binary millisecond pulsar, an intermittent pulsar, and a pulsar with an interpulse. No new relativistic binary pulsars have been discovered.

Searches for relativistic binaries are already underway in the HTRU pulsar surveys (Ng 2011, Ng et al. in prep). The low-latitude portion of the survey will cover a thin strip ($|b| < 3.5^\circ$) along the Galactic plane with integration times of over 70 minutes. For these long integration times acceleration searches will not be sensitive to the most relativistic binary pulsars; higher order effects will need to be taken into account (see Section 6.3.3). Unfortunately, it can be shown that searches in these higher order effects are still computationally prohibitive for long integrations. Assuming a sampling interval of 128 μs and using step-sizes in acceleration and jerk given by Equations 3 and 6 respectively, corrections for the effects of both acceleration and jerk in a 'Double Pulsar like' system would require of the order of $\sim 10^7$ trials per DM trial for a 70 minute observation (c.f. 59 acceleration trials per DM as in this work). For the analysis of the low-latitude HTRU data, either incoherent methods such as stack searches (Eatough et al. in prep), or coherent acceleration searches of different length but shorter segments of the original 70 minute observations should be performed (Ng et al. in prep).

Because of the limitations of the acceleration search performed in this work, a full re-processing of the PMPS has been conducted utilizing the Einstein@Home network[13]. This search applies matched filters to coherently de-modulate the data based on a number of Keplerian orbital templates, which allows the full integration length to be searched (Knispel et al. in prep).

The discovery and timing of highly relativistic binary pulsars is one of the key science projects of the SKA (Cordes et al. 2004). As well as offering highly rewarding discoveries, current searches for such systems, both in archival data and in data from the latest pulsar surveys, will provide considerable information on the binary parameter space still to be searched in, and on the strategy of future pulsar surveys.

ACKNOWLEDGEMENTS

This research was partly funded by grants from the Science & Technology Facilities Council. The Parkes radio telescope is part of the Australia Telescope National Facility which is funded by the Commonwealth of Australia for operation as a National Facility managed by CSIRO. This work was based on observations with the 100-m telescope of the MPIfR (Max-Planck-Institut für Radioastronomie) at Effelsberg. We would like to thank Xu D. D. for many useful discussions about the ideas presented here. We thank C. Jordan and the staff of the Parkes observatory for observational help at Jodrell Bank and Parkes respectively. We also wish to thank E. F. Keane for manuscript reading and A. Noutsos for useful discussions. The authors kindly wish to thank A. Forti and The University of Manchester High Energy Physics group for use of the TIER2 computing facility.

[13] http://einstein.phys.uwm.edu/

REFERENCES

Belczynski K., Benacquista M., Bulik T., 2010, ApJ, 725, 816
Belczynski K., Kalogera V., Bulik T., 2002, ApJ, 572, 407
Bethe H. A., Brown G. E., 1998, ApJ, 506, 780
Brady P. R., Creighton T., 2000, Phys. Rev. D., 61, 082001
Breton R. P. et al., 2008, Science
Burgay M. et al., 2003, Nature, 426, 531
Camilo F., Lorimer D. R., Freire P., Lyne A. G., Manchester R. N., 2000, ApJ, 535, 975
Cordes J. M., Kramer M., Lazio T. J. W., Stappers B. W., Backer D. C., Johnston S., 2004, New Astronomy Review, 48, 1413
Cordes J. M., Lazio T. J. W., preprint (arXiv:astro-ph/0207156)
Damour T., Esposito-Farèse G., 1998, Phys. Rev. D, 58, 1
Damour T., Ruffini R., 1974, C. R. Acad. Sc. Paris, Serie A, 279, 971
Dhurandhar S. V., Vecchio A., 2001, Phys. Rev. D, 63, 122001
Eatough R. P., 2009, Ph.D. thesis, University of Manchester
Eatough R. P., Keane E. F., Lyne A. G., 2009, MNRAS, 395, 410
Eatough R. P., Molkenthin N., Kramer M., Noutsos A., Keith M. J., Stappers B. W., Lyne A. G., 2010, MNRAS, 407, 2443
Faulkner A. J., 2004, Ph.D. thesis, University of Manchester
Faulkner A. J. et al., 2005, ApJ, 618, L119
Faulkner A. J. et al., 2004, MNRAS, 355, 147
Freire P. C. C. et al., 2012, MNRAS, 423, 3328
Hobbs G. et al., 2004, MNRAS, 352, 1439
Johnston H. M., Kulkarni S. R., 1991, ApJ, 368, 504
Kalogera V. et al., 2004, ApJ, 601, L179
Kaspi V. M. et al., 2000, ApJ, 543, 321
Keane E. F., Kramer M., Lyne A. G., Stappers B. W., McLaughlin M. A., 2011, MNRAS, 838
Keane E. F., Ludovici D. A., Eatough R. P., Kramer M., Lyne A. G., McLaughlin M. A., Stappers B. W., 2010, MNRAS, 401, 1057
Keith M. J., Eatough R. P., Lyne A. G., Kramer M., Possenti A., Camilo F., Manchester R. N., 2009, MNRAS, 395, 837
Keith M. J. et al., 2010, MNRAS, 409, 619
Kim C., Kalogera V., Lorimer D. R., 2003, ApJ, 584, 985

Kramer M., 1998, ApJ, 509, 856
Kramer M., Backer D. C., Cordes J. M., Lazio T. J. W., Stappers B. W., Johnston S., 2004, New Astronomy Reviews, 48, 993
Kramer M. et al., 2003, MNRAS, 342, 1299
Kramer M., Lyne A. G., O'Brien J. T., Jordan C. A., Lorimer D. R., 2006a, Science, 312, 549
Kramer M. et al., 2006b, Science, 314, 97
Lipunov V. M., Bogomazov A. I., Abubekerov M. K., 2005, MNRAS, 359, 1517
Liu K., Wex N., Kramer M., Cordes J. M., Lazio T. J. W., 2012, ApJ, 747, 1
Lorimer D. R. et al., 2006a, MNRAS, 372, 777
Lorimer D. R., Kramer M., 2005, Handbook of Pulsar Astronomy. Cambridge University Press
Lorimer D. R. et al., 2006b, ApJ, 640, 428
Lyne A. G., Smith F. G., 2006, Pulsar Astronomy, 3rd ed. Cambridge University Press, Cambridge
Maciesiak K., Gil J., Ribeiro V. A. R. M., 2011, MNRAS, 414, 1314
Manchester R. N. et al., 2010, ApJ, 710, 1694
Manchester R. N. et al., 2001, MNRAS, 328, 17
McLaughlin M. A. et al., 2006, Nature, 439, 817
Middleditch J., Kristian J., 1984, ApJ, 279, 157
Morris D. J. et al., 2002, MNRAS, 335, 275
Nelemans G., Yungelson L. R., Portegies Zwart S. F., 2001, A&A, 375, 890
Ng C., 2011, in 41st Young European Radio Astronomers Conference
Osłowski S., Bulik T., Gondek-Rosińska D., Belczyński K., 2011, MNRAS, 413, 461
Pfahl E., Podsiadlowski P., Rappaport S., 2005, ApJ, 628, 343
Phinney E. S., 1992, Philos. Trans. Roy. Soc. London A, 341, 39
Portegies Zwart S. F., Yungelson L. R., 1998, A&A, 332, 173
Ransom S. M., Cordes J. M., Eikenberry S. S., 2003, ApJ, 589, 911
Sipior M. S., Portegies Zwart S., Nelemans G., 2004, MNRAS, 354, L49
Sipior M. S., Sigurdsson S., 2002, ApJ, 572, 962
Smits R., Kramer M., Stappers B., Lorimer D. R., Cordes J., Faulkner A., 2009a, A&A, 493, 1161
Smits R., Lorimer D. R., Kramer M., Manchester R., Stappers B., Jin C. J., Nan R. D., Li D., 2009b, A&A, 505, 919
Stappers B. W. et al., 2011, A&A, 530, A80
Taylor J. H., Huguenin G. R., 1969, Nature, 221, 816
Taylor J. H., Weisberg J. M., 1989, ApJ, 345, 434
Thorsett S. E., Chakrabarty D., 1999, ApJ, 512, 288
van Leeuwen J., Stappers B. W., 2010, A&A, 509, A7
Voss R., Tauris T. M., 2003, MNRAS, 342, 1169
Weltevrede P., Johnston S., 2008, MNRAS, 387, 1755
Wex N., Kopeikin S., 1999, ApJ, 513, 388
Wood K. S. et al., 1991, ApJ, 379, 295